NJC

PAPER

View Article Online
View Journal | View Issue

Cite this: *New J. Chem.*, 2014, **38**, 1627

Rhodamine-based molecular clips for highly selective recognition of Al^{3+} ions: synthesis, crystal structure and spectroscopic properties†

Anamika Dhara,[a] Atanu Jana,*[a] Nikhil Guchhait,*[a] Prasanta Ghosh[b] and Susanta K. Kar*[a]

Received (in Victoria, Australia) 20th November 2013,
Accepted 30th January 2014

DOI: 10.1039/c3nj01447a

www.rsc.org/njc

A novel fluorescent chemosensor based on a rhodamine derivative (**L**) was designed, synthesized, and used as a selective Al^{+3} ion sensor. Upon addition of Al^{3+} to an aqueous-acetonitrile solution of **L**, the development of a strong fluorescence signal by a chelation-enhanced fluorescence (CHEF) process was observed with an attractive glowing orange emission. This sensor shows high selectivity towards Al^{3+} ions in the presence of other competing metal ions. The fluorescence quantum yield of **L**–Al^{3+} (Φ_f = 0.30) was found to be very high compared to the bare ligand. The limit of detection (LOD) of Al^{3+} ions was calculated to be 2×10^{-8} M by fluorescence titration. The 1:1 binding stoichiometry of the metal complex was established by combined UV-vis, fluorescence and TOF-MS spectroscopy.

Introduction

The recognition and sensing of biologically and environmentally important species have emerged as a significant goal in the field of chemical sensors in recent years, since they allow nondestructive and prompt detection of the species (cations or anions) by a simple fluorescence enhancement (turn-on) or quenching (turn-off) response.[1] Aluminum is the third most abundant metallic element in the earth's crust, which is found in water and most biological tissues in its ionic form Al^{3+}. The amount of free Al^{3+} in the surface water is increased by leaching from soil due to acid rain. It is toxic to plants and kills fish in acidified water.[2] The World Health Organization (WHO) recommended the average daily human intake of Al^{3+} of around 3–10 mg and the weekly tolerable dietary intake of 7 mg kg^{-1} body weight.[3] The widespread use of aluminum around us in the modern society are in water treatment, food additives, medicines, and of course, in the production of cooking utensils, aluminum foil, *etc.* Al^{3+} toxicity causes microcytic hypochromic anemia, Al-related bone disease (ARBD), encephalopathy, neuronal disorder leading to dementia, myopathy, and also affects the absorption of iron in blood, causing anemia. In addition, the toxicity of aluminum causes damage to the central nervous system, is suspected to be involved in neurodegenerative diseases such as Alzheimer's and Parkinson's and is responsible for intoxication in hemodialysis patients.[4] In the biosphere, the detection and estimation of Al^{3+} levels have significant importance for human health. Recently, the design and construction of chemosensors with high selectivity and sensitivity towards Al^{3+} have become the focus in numerous studies in the field of supramolecular chemistry. The poor coordination ability, strong hydration ability, and the lack of spectroscopic characteristics of Al^{3+} have hindered development of a suitable fluorescence sensor compared to other metal ions.[5] Practically, Al^{3+} is a hard-acid; it is found that Al^{3+} prefers a coordination sphere containing N and O as hard-base donor sites.[6] As a result, most of the reported Al^{3+} sensors contain mixed nitrogen and oxygen donor sites. So, the design and synthesis of highly sensitive and selective fluorescent chemosensors for Al^{3+} is still in great demand.

The rhodamine moiety has been used widely in the field of chemosensors, especially as a chemodosimeter, given its fluorescence OFF–ON behavior resulting from its unique structural architecture and properties. In general, the spirolactam form of rhodamine derivatives is found to be nonfluorescent, whereas its ring opened amide system gives rise to a strong fluorescence emission.[7] Furthermore, the rhodamine fluorophore exhibits a longer wavelength emission (over 550 nm), often serving as a sensor for the analyte to avoid the influence of background fluorescence (below 500 nm).[8] Rhodamine spirolactam based chemosensors are attractive because of their excellent photophysical properties, such as long absorption

[a] *Department of Chemistry, University College of Science, University of Calcutta, 92, A.P.C. Road, Kolkata, 700 009, India. E-mail: skkar_cu@yahoo.co.in; Fax: +91 33 23519755; Tel: +91 33 24322936*

[b] *Department of Chemistry, R. K. Mission Residential College, Narendrapur, Kolkata-103, India*

† Electronic supplementary information (ESI) available. CCDC 973400. For ESI and crystallographic data in CIF or other electronic format see DOI: 10.1039/c3nj01447a

and emission wavelengths elongated to the visible region, high fluorescence quantum yield, and a large absorption coefficient.[9]

Here, we report a novel rhodamine-based spirolactam derivative (**L**) as a chemosensor for Al^{3+} [6,10] where the binding phenomena could be probed through binding induced changes in the electronic spectral pattern *via* the chelation enhanced fluorescence (CHEF)[6,10d] effect in the presence of Al^{3+} ions. Interestingly, binding of these metal ions to **L** causes color changes, which could also be detected by the "naked eye". Most interestingly, the fluorescence emission at 581 nm for rhodamine is relatively unaffected in the pH range between 4.8 and 9.2. Therefore, we have speculated that the introduction of the dihydroxybenzaldehyde receptor to a rhodamine-based probe would (1) increase its affinity towards Al^{3+} ions in aqueous–acetonitrile media, (2) quickly induce the fluorescent and color responses, that is, realize the real-time detection, (3) improve the selectivity, and (4) recognize reversible binding to Al^{3+} and hence can be useful as a potential chemosensor material. To the best of our knowledge, there are very few reports on aluminum sensors based on rhodamine dyes through the spirocyclic ring-opening mechanism.[11] In this work we report a new molecule for selective detection of Al^{3+} ions fluorogenically as well as colorimetrically.

Results and discussion

Rhodamine B hydrazide was synthesized following a literature method[12] and characterized by ^{1}H NMR spectra, mass data, and FT-IR. It was then condensed with 2,3-dihydroxybenzaldehyde in methanol to form **L** in 71% yield (Scheme 1). The structure of compound **L** was confirmed by its spectroscopic, analytical data (^{1}H NMR, ^{13}C NMR, ESI-MS, FT-IR, and Fig. S1–S4, ESI†) and X-ray crystal structure analysis (Fig. 1). Single crystals of **L** were obtained by slow evaporation of the methanol solution (Tables 1 and 2).

We have carried out UV-vis titration experiments to understand the nature of binding of **L** to Al^{3+}. The chemosensor **L** (10 μM) in CH_3CN–H_2O (8 : 2, v/v) buffered with 2-[4-(2-hydroxyethyl)piperazin-1-yl]ethanesulfonic acid (HEPES), pH = 7.2 showed an absorption maximum at 347 nm, suggesting that the spirolactam ring of the rhodamine B unit preferred its ring-closed state under these conditions. The selectivity of **L** has been checked with different biologically important metal ions *e.g.*, Na^+, Mg^{2+}, Hg^{2+}, Cu^{2+}, Pb^{2+}, Zn^{2+}, Mn^{2+}, Fe^{3+}, Co^{2+}, Ni^{2+}, Cd^{2+}, Cr^{3+}, In^{3+}, Ga^{3+} and Al^{3+} in

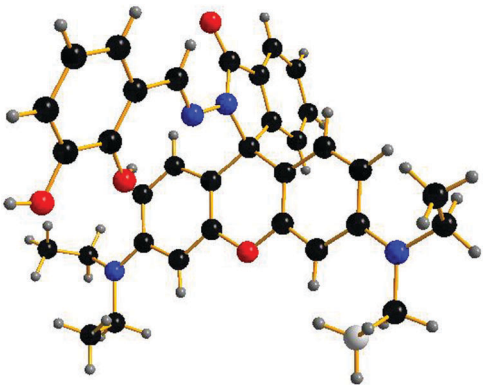

Fig. 1 Crystal structure of **L** (different color balls indicate different atoms; blue = N, red = O, black = C and grey = H).

CH_3CN–aqueous (8 : 2, v/v) buffered with HEPES, pH = 7.2. A significant change in the UV-vis spectral pattern was observed only in the presence of Al^{3+} among all the other metal ions used (Fig. S7, ESI†). Upon gradual addition of Al^{3+} ions (0–100 μM) to chemosensor **L** (10 μM) in CH_3CN–H_2O (8 : 2, v/v), a concomitant red shift in the spectral position at 554 nm was observed along with an increase in the absorption intensity. The emergence of the absorption band at 554 nm was due to the opening of the spirolactam ring of the rhodamine moiety along with a color change from colorless to deep magenta (Fig. 2). As depicted in the inset of Fig. 2, the absorbance at the 554 nm band as a function of Al^{3+} concentration predicted a 1 : 1 stoichiometry for the complex between **L** and Al^{3+} ions. The association constant[13] between **L** and the Al^{3+} ion was calculated from the absorption titration result and was found to be 2.11×10^3 M^{-1} at 25 °C (Fig. 3). Under the same conditions, addition of other metal ions did not cause any discernible changes. This unique selectivity of **L** towards Al^{3+} can be explained in terms of the absolute hardness (η), defined as $\eta = (I + A)/2$, where I and A are the ionization potential and proton affinity, respectively. Namely, it was reported by Paar and Pearson that Al^{3+} is the hardest acid among all the cations considered in this study[14] (Scheme 2). The color of the solution was significantly changed from deep magenta to bright orange when illuminated with a hand-held UV lamp (Fig. 4). So it could easily be detected by the "naked-eye" without the need of any other instrumental assistance.

The fluorescence spectrum of **L** (10 μM) in CH_3CN–H_2O (8 : 2, v/v) buffered with HEPES, pH = 7.2, exhibited an emission band at 542 nm when excited at 554 nm. Upon interaction with

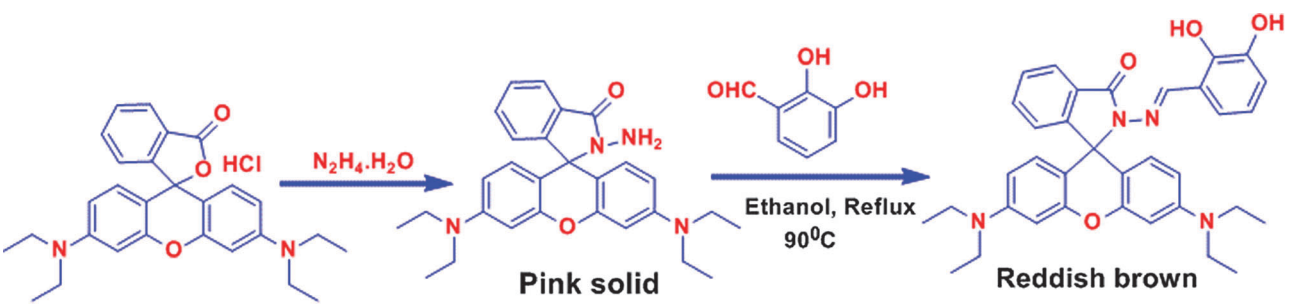

Scheme 1 Synthesis of chemosensor **L**.

Table 1 Crystallographic data of **L**

Identification code	**L**
Empirical formula	$C_{35}H_{36}N_4O_4$
Formula weight	576.68
Temperature, K	293(2)
Wavelength, Å	0.710730
Crystal system	Monoclinic
Space group	*P*21
a, Å	9.3382(4)
b, Å	27.1749(12)
c, Å	12.0639(5)
α, °	90.00
β, °	102.556(2)
γ, °	90.00
Volume, Å^3	2988.2(2)
Z	4
Density (calc), Mg m^{-3}	1.282
Abs. coefficient, mm^{-1}	0.085
F(000)	1224
Crystal size, mm^3	0.05 × 0.03 × 0.02
θ Range (°) for data collection	1.5–28.3
Independent reflections (R_{int})	38 950, 13 485, 0.045
Absorption correction	MULTI-SCAN
Refinement method	Full-matrix least squares on F^2
Data/restraints/parameters	13485/1/755
Goodness-of-fit on F^2	1.121
R_1, wR_2 [$I > 2\sigma(I)$]	0.0775, 0.2308
Flack's parameter	0.5(15)
Largest difference peak and hole (e Å^{-3})	−0.56, 0.70
CCDC number	973400

Table 2 Selected bond distances (Å) and angles (°) in **L**

Selected bonds	Value (Å)
O4–C92	1.219(5)
N13–N14	1.366(5)
C122–C123	1.388(7)
O16–C123	1.336(6)
Selected angles	**Value (°)**
O4–C92–N13	125.2(4)
N13–N14–C121	122.5(4)
C121–C122–C123	122.5(4)

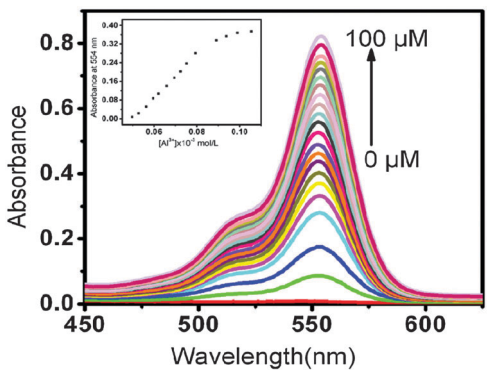

Fig. 2 UV-vis spectra of chemosensor **L** (10 μM) in CH_3CN–H_2O (8 : 2, v/v) with HEPES buffer, pH = 7.2 at 25 °C, in the presence of different amounts of Al^{3+} ions (0–100 μM). Inset: absorbance at 554 nm as a function of Al^{3+} concentration, indicating a 1 : 1 metal–ligand ratio.

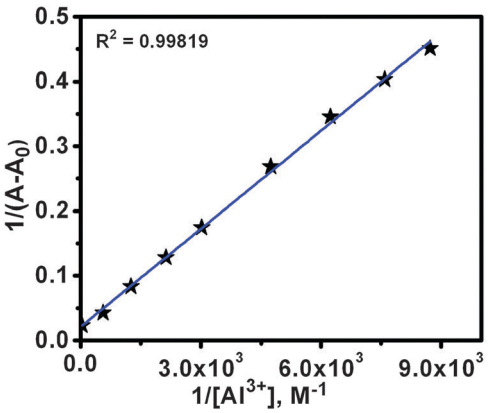

Fig. 3 Benesi–Hildebrand plot of chemosensor **L** (10 μM) in CH_3CN–H_2O (8 : 2, v/v) with HEPES buffer, pH = 7.2 at 25 °C, absorbance at 554 nm assuming a 1 : 1 stoichiometry between **L** and Al^{3+}.

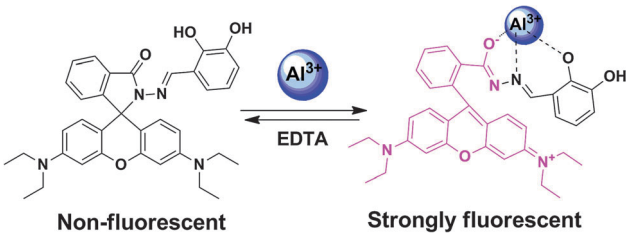

Scheme 2 Proposed binding mode of chemosensor **L** with Al^{3+}.

various metal ions *e.g.*, Al^{3+}, Cr^{3+}, In^{3+}, Ga^{3+}, Na^+, Mg^{2+}, Pb^{2+}, Hg^{2+}, Fe^{3+}, Cu^{2+}, Ni^{2+}, Co^{2+}, Mn^{2+}, Cd^{2+} and Zn^{2+} a much weaker spectral response was observed relative to Al^{3+} at the same concentration (Fig. 5a). During sequential titration (0–100 μM of Al^{3+}), the emission band peaked up at 581 nm which was attributed to delocalization in the xanthene moiety of the rhodamine and hence emission intensity was increased significantly (Fig. 6). The observed fluorescence occurred due to the metal binding event induced an electronic rearrangement within the dye that opened the spirolactam and yielded a fully conjugated rhodamine dye. The solution showed an intense orange fluorescence, with an approximately 15-fold enhancement in the fluorescence intensity at 581 nm. The inset in Fig. 6 shows the dependence of the emission intensity at 581 nm on increase of Al^{3+} ion concentration. This fact means that **L** could be used as an 'off–on' fluorescent chemosensor for Al^{3+}. Relative fluorescence enhancement of **L** in the absence and presence of various other metal ions and thereby its selectivity for Al^{3+} are shown in Fig. 5b.

To investigate the recognition ability between **L** and the Al^{3+} ion, both Job's plot[15] and Benesi–Hildebrand plot[13] experiments were carried out to determine the binding stoichiometry of the **L**–Al^{3+} complex. The absorption intensity varies through a maximum at a molar fraction of about 0.5 of Al^{3+}, indicating a 1 : 1 stoichiometry and this is the most possible case of binding of Al^{3+} with **L** (Fig. 7). To confirm further the stoichiometry between **L** and the Al^{3+} ion, TOF-MS analysis was conducted (Fig. S5, ESI†). A mass peak at *m*/*z* 729.09 corresponding to **L**·Al(SO_4)(OMe) is indicative of the formation of a 1 : 1 complex.

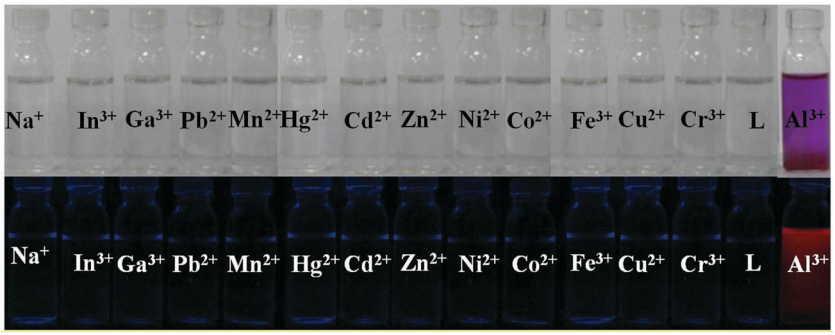

Fig. 4 Photographs of chemosensor **L** (10 μM) in $CH_3CN–H_2O$ (8 : 2, v/v) with HEPES buffer, pH = 7.2 at 25 °C, in the presence of different metal ions (100 μM) under (a) visible light and (b) UV light.

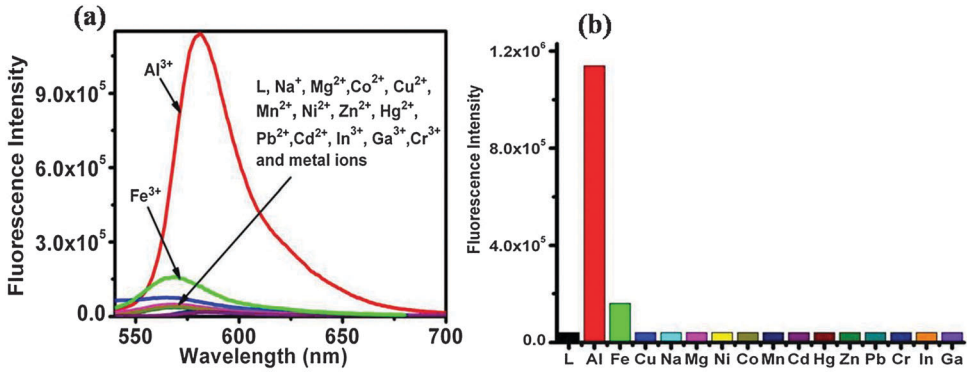

Fig. 5 Fluorescence spectra (excitation at 554 nm) of **L** (10 μM) in $CH_3CN–H_2O$ (8 : 2, v/v) with HEPES buffer, pH = 7.2 at 25 °C, with addition of biologically important metal ions *e.g.*, Al^{3+}, Cr^{3+}, In^{3+}, Ga^{3+}, Na^{+}, Mg^{2+}, Pb^{2+}, Hg^{2+}, Fe^{3+}, Cu^{2+}, Ni^{2+}, Co^{2+}, Mn^{2+}, Cd^{2+} and Zn^{2+} (100 μM).

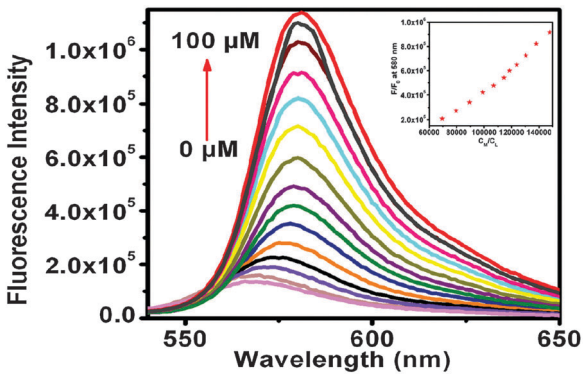

Fig. 6 Emission spectra of chemosensor **L** (10 μM) in the presence of increasing concentrations of Al^{3+} (0, 15, 25, 30, 35, 40, 45, 50, 55, 60, 65, 70, 75, 80, and 100 μM) in $CH_3CN–H_2O$ (8 : 2, v/v) with HEPES buffer, pH = 7.2 at 25 °C. Excitation was performed at 554 nm. Inset: fluorescence intensity at 581 nm as a function of Al^{3+} concentration.

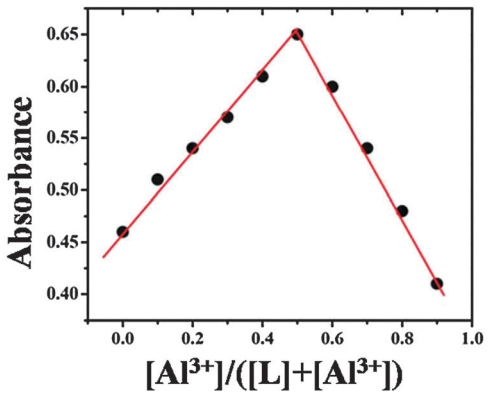

Fig. 7 Absorbance at 554 nm of **L** (10 μM) and Al^{3+} with a total concentration of 100 μM in $CH_3CN–H_2O$ (8 : 2, v/v) with HEPES buffer, pH = 7.2 at 25 °C, indicating a 1 : 1 metal–ligand ratio.

From the emission intensity data, the association constant (K)[13] of **L** with Al^{3+} was observed to be 2.56×10^3 M^{-1}, indicating strong binding of **L** with the Al^{3+} ion with 1 : 1 stoichiometry (Fig. 8). Values thus evaluated using two different spectroscopic techniques were in good agreement.

To check the practical ability of chemosensor **L** as a selective Al^{3+} ion fluorescent chemosensor, we have carried out competitive experiments in the presence of Al^{3+} ions mixed with other different metal ions (Cr^{3+}, In^{3+}, Ga^{3+}, Na^{+}, Mg^{2+}, Pb^{2+}, Hg^{2+}, Fe^{3+}, Cu^{2+}, Ni^{2+}, Co^{2+}, Mn^{2+}, Cd^{2+} and Zn^{2+}). The fluorescence response of the **L**–Al^{3+} system remains the same by comparison with or without the other metal ions (Fig. 9). These findings confirmed the selectivity and effective interaction of probe **L** with Al^{3+}. For practical applications, the detection limit of **L** was also estimated. The fluorescence titration profile of **L** (10 μM) with Al^{3+} demonstrated that the detection limit[16] of Al^{3+} is 2×10^{-8} M which is far below the WHO acceptable limit (0.05 mg L^{-1} or 1.85 μM of Al^{3+}) in drinking water (Fig. 10).

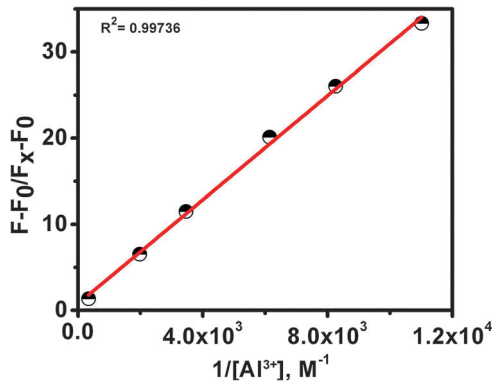

Fig. 8 Benesi–Hildebrand plot ($[F - F_0/F_x - F_0]$ *vs.* $1/[Al^{3+}]$) for complexation between chemosensor **L** and Al^{3+} derived from emission spectral data.

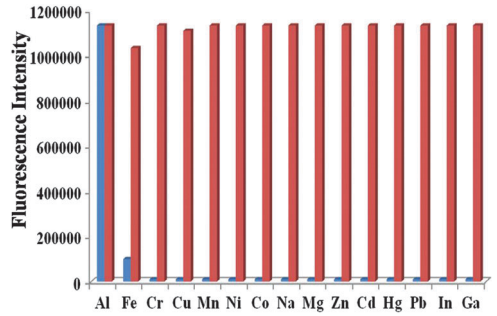

Fig. 9 Fluorescence responses of **L** (10 μM) to various cations in CH_3CN–H_2O (8 : 2, v/v) using HEPES buffer, pH = 7.2 at 25 °C. The blue bars represent the emission intensities of **L** in the presence of cations of interest (100 μM). The red bars represent the change of the emission that occurs upon the subsequent addition of Al^{3+} to the above solution. The intensities were recorded at 581 nm.

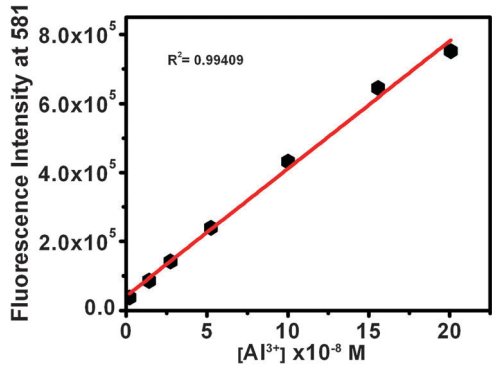

Fig. 10 Determination of the detection limit of Al^{3+} by **L** (10 μM) in CH_3CN–H_2O (8 : 2, v/v) using HEPES buffer, pH = 7.2 at 25 °C, (λ_{ex} = 554 nm and λ_{em} = 581 nm).

In order to gain insight into the sensing mechanism, ^1H NMR titration has been performed by 1 equiv. addition of Al^{3+} to the DMSO-d_6 solution of **L** (Fig. 11). Upon addition of 1 equiv. of Al^{3+}, the i proton of **L** has gradually shifted downfield from 8.85 (free **L**) to 9.03 ppm. Downfield shifts of both a and b in the *N*,*N*-diethyl group of **L** clearly indicate that Al^{3+} induces the formation of a delocalised xanthene moiety of rhodamine B. All other protons of **L** *viz.* c, d, e, f, g, and h have been shifted downfield after interaction with Al^{3+}. Further, IR spectra of chemosensor **L** with Al^{3+} ions also confirm the proposed mechanism (Fig. S6, ESI†). Upon addition of 1 equiv. of Al^{3+}, the characteristic carbonyl amide stretching frequency shifts from 1690 cm^{-1} in **L** to 1662 cm^{-1} in the complex, indicating coordination of carbonyl oxygen with Al^{3+}. These findings clearly support the ring-opening mechanism.

Reversible binding of Al^{3+} to **L** was also established through spectral studies in the presence of Na_2EDTA in CH_3CN–H_2O solution. Upon addition of EDTA (excess) to the mixture of **L** (10 μM) and Al^{3+} in CH_3CN–H_2O (8 : 2, v/v), the color of the solution disappeared instantly. If Al^{3+} was added to the system again, the signal is almost completely recovered with solution changing from colorless to pink (Fig. S8, ESI†). These findings indicate that **L** was a reversible fluorescent probe for Al^{3+}. Fluorescence quantum yield (Φ_{fs})[17] of **L** in the free and Al^{3+}-bound state was found to be 0.02 and 0.30 respectively.

The enhancement of fluorescence of **L** upon binding with Al^{3+} has been supported by the results obtained from fluorescence decay measurements, using the Time Correlated Single Photon Counting (TCSPC) technique (Fig. 12). The fluorescence decay of **L** was fitted with triexponential function with time constant of (τ_1) 1.2 ns (15.5%), (τ_2) 4.38 ns (4.5%) and (τ_3) 0.49 ns (80%). Upon binding with Al^{3+} ions the same fluorescence decay was observed at (τ_1) 3.05 ns (20%), (τ_2) 1.63 ns (3%) and (τ_3) 0.04 ns (76%) (χ^2 = 1.08 and 1.30) in CH_3CN–H_2O (8 : 2 v/v) using HEPES buffer, pH = 7.2 at 25 °C. The average fluorescence lifetime of the bare molecules (2.66 ns) was decreased in the complex (2.07 ns); this was due to the opening of the spirolactum ring (Table S1, ESI†). Upon addition of Al^{3+} to the chemosensor (**L**) formation of a tight binding complex occurs (as observed from the higher binding constant) along with the opening of the spirolactam ring to convert the free (hanging) rhodamine B part of the complex, thereby increasing non-radiative decay channels and as a result the average lifetime decreased.

To study the practical applicability, the effect of pH on the fluorescence response of the new chemosensor **L** towards Al^{3+} has also been investigated. Experimental results show that for free **L**, under acidic conditions (pH < 3), an obvious fluorescence off–on (Fig. S9, ESI†) situation appears due to the formation of the open-ring state because of the strong protonation, and it shows a fluorescence quenching effect upon addition of Al^{3+}. In the pH range from 4.8 to 9.2, neither the color nor the fluorescence (excited at 554 nm) characteristics of rhodamine could be observed for **L**, suggesting that the spirocyclic form was still preferred in this range.

Conclusion

In summary, we have developed a novel turn-on fluorescent chemosensor based on a rhodamine–dihydroxybenzaldehyde conjugate. The sensor **L** displays an excellent selectivity and high sensitivity toward the detection of Al^{3+} in CH_3CN–H_2O over a wide range of tested metal ions with remarkably enhanced fluorescent intensity and also shows a clear color change from colorless to deep

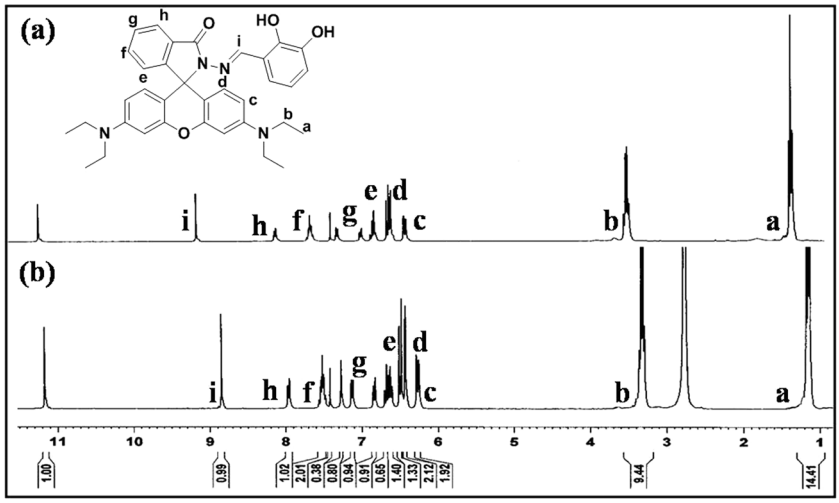

Fig. 11 ^{1}H NMR spectra of **L** and Al^{3+} ions (DMSO-d_6). (b) **L** only (a) **L** with 1 equiv. of Al^{3+}.

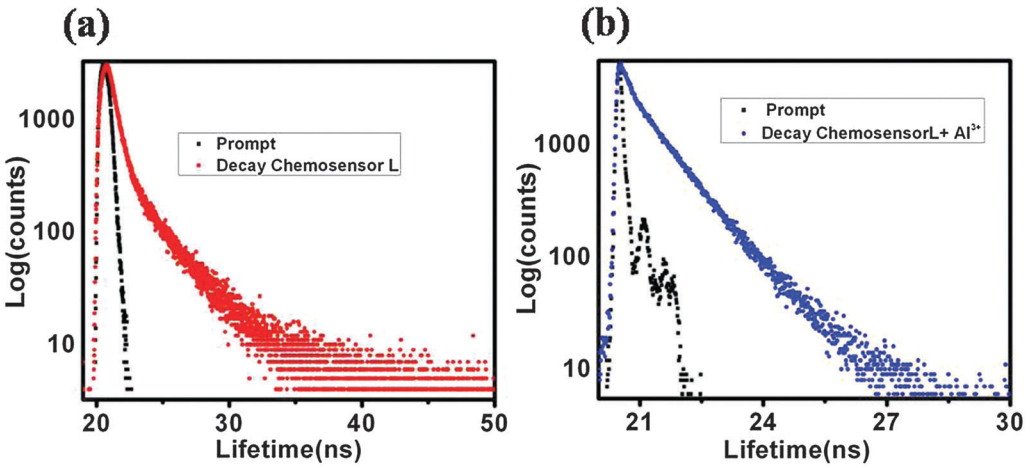

Fig. 12 (a) Time-resolved fluorescence decay of **L** (red) in the absence of any metal ion with the excitation source of λ_{ext} = 340 nm while monitored at λ_{em} = 581 nm in CH_3CN–H_2O (8 : 2, v/v) media. (b) Emission decay for **L** (blue) in the presence of the aluminum ion with the excitation source of λ_{ext} = 450 nm while monitored at λ_{em} = 581 nm in CH_3CN–H_2O (8 : 2, v/v) media.

magenta. A comparison of the present probe with other existing Al^{3+} sensitive "turn-on" fluorescent probes reveals that it is very competitive and somewhat better than others in respect of all the parameters. The present probe is relatively cheap as it involves a facile two step reaction with the commercially available much cheaper chemicals. Under UV light illumination, one can visually detect even 2×10^{-8} M Al^{3+} in aqueous–acetonitrile buffer solution using this sensor without the aid of any sophisticated instruments. Thus the chemosensor **L** is able to serve as a 'naked eye' chemosensor for Al^{3+} ions. We believe that **L** can be used for many practical applications in chemical, environmental and biological systems.

Experimental section

General information

The solvents and reagents were purchased from Sigma-Aldrich commercial sources and were used without any further purification. The solvents were distilled prior to use. The rhodamine B hydrazide was prepared by literature methods. Elemental analyses (carbon, hydrogen and nitrogen) were done using a Perkin-Elmer CHN analyzer 2400. Melting points were determined using a Buchi 530 melting apparatus. ^{1}H and ^{13}C NMR spectra were recorded on Bruker Avance II 500 MHz and Bruker Avance 300 MHz spectrometers in DMSO-d_6 and $CDCl_3$. Mass spectra were recorded in methanol solvent on a Qtof Micro YA263. The electronic spectra were recorded in CH_3CN–H_2O solution on a Hitachi model U-3501 spectrophotometer. IR spectra (KBr pellet, 400–4000 cm^{-1}) were recorded on a Perkin-Elmer model 883 infrared spectrophotometer. Emission spectra were measured using a Perkin Elmer (Model LS-50B) fluorimeter.

Time resolved spectral measurements

Fluorescence lifetimes were measured by the method of Time Correlated Single-Photon counting (TCSPC) using a HORIBA

Jobin Yvon Fluorocube-01-NL fluorescence lifetime spectrometer. The sample was excited using a nanosecond laser diode at 340 nm and 450 nm and the signals were collected at the magic angle of 54.7°.[18] The typical time resolution of our experimental set-up is ~800 ps. The decays were deconvoluted using DAS-6 decay analysis software. The acceptability of the fits was judged by χ^2 criteria and visual inspection of the residuals of the fitted function to the data. Mean (average) fluorescence lifetimes were calculated using the following eqn (1):

$$\tau_{av} = \frac{\sum \alpha_i \tau_i^2}{\sum \alpha_i \tau_i} \quad (1)$$

in which α_i is the pre-exponential factor corresponding to the ith decay time constant, τ_i.

Fluorimetric analysis

For measurement of the quantum yields (Φ) of **L** and its complex, we recorded the absorbance of the compounds in CH_3CN–H_2O solution. The emission spectra were recorded using the maximal excitation wavelengths, and the integrated areas of the fluorescence-corrected spectra were measured. The fluorescence quantum yield was measured using rhodamine 6G (Φ = 0.95 in ethanol) as the reference[19] according to the following equation:[20]

$$\Phi_X = \Phi_S \times (I_X/I_S) \times (A_S/A_X) \times (\eta_X/\eta_S)^2 \quad (2)$$

where X and S indicate the unknown and standard solution, respectively, Φ is the quantum yield, I is the integrated area under the fluorescence spectra, A is the absorbance and η is the refractive index of the solvent.

Association constant

(i) Calculation of the association constant using spectrophotometric titration data. The association constant for the formation of the complex, [Al^{3+}–L] was evaluated using the Benesi–Hildebrand (B–H) plot

$$1/(A - A_0) = 1/\{K(A_{max} - A_0)C\} + 1/(A_{max} - A_0) \quad (3)$$

where A_0 is the absorbance of **L** at absorbance maxima (λ = 554 nm), A is the observed absorbance at that particular wavelength in the presence of a certain concentration of the metal ion (C), A_{max} is the maximum absorbance value that was obtained at λ = 554 nm (for Al^{3+}) during titration with varying [C], K is the association constant (M^{-1}) and was determined from the slope of the linear plot, and [C] is the concentration of the Al^{3+} ion added during titration studies. The goodness of the linear fit of the B–H plot of $1/(A - A_0)$ *vs.* $1/[Al^{3+}]$ for 1 : 1 complex formation confirms the binding stoichiometry between **L** and Al^{3+}.

(ii) Calculation of the association constant using emission titration data. Association constant was calculated using the Benesi–Hildebrand equation:

$$1/\Delta F = 1/\Delta F_{max} + (1/K[C])(1/\Delta F_{max}) \quad (4)$$

Here $\Delta F = F_x - F_0$ and $\Delta F_{max} = F - F_0$, where F_0, F_x, and F are the emission intensities of **L** considered in the absence of Al^{3+}, at an intermediate Al^{3+} concentration, and at a concentration of complete interaction, respectively, at 581 nm and where K is the binding constant and [C] the Al^{3+} concentration. The plot of $(F - F_0)/(F_x - F_0)$ against $[C]^{-1}$ and the association constant (K) was obtained using the intercept/slope ratio.

Calculation of the detection limit

The detection limit (DL) of **L** for Al^{3+} was determined using the following equation:

$$DL = K \times Sb/S \quad (5)$$

where K = 2 or 3 (we take 3 in this case), Sb is the standard deviation of the blank solution and S is the slope of the calibration curve.

General procedures of spectra detection

Stock solutions (2×10^{-3} M) of different metal ions such as, Al^{3+}, Cr^{3+}, In^{3+}, Ga^{3+}, Na^{+}, Mg^{2+}, Pb^{2+}, Hg^{2+}, Fe^{3+}, Cu^{2+}, Ni^{2+}, Co^{2+}, Mn^{2+}, Cd^{2+} and Zn^{2+} were prepared. High concentration of the stock solutions chemosensor **L** (10 μM) was prepared in acetonitrile. Before spectroscopic measurements, the solution of **L** was freshly prepared by diluting the high concentration stock solution to the concentration of desirable solution. The suspension solutions of **L** were prepared by dispersing the fine powder in water. Each time a 2 mL solution of **L** was filled in a quartz cell of 1 cm optical path length, and different stock solutions of cations were added into the quartz cell gradually by using a micro-pipette. The volume of cationic stock solution added was less than 100 L with the purpose of keeping the total volume of testing solution without obvious change. All the spectroscopic measurements were performed at least in triplicate and averaged.

Synthesis of chemosensor L

Rhodamine B hydrazide was synthesized following a literature procedure.[12] To a solution of 2,3-dihydroxybenzaldehyde (0.151 gm, 1.095 mmol) in methanol (10 mL) was added rhodamine B hydrazide (0.5 gm, 1.095 mmol) in methanol (10 mL). The resulting solution was heated to reflux at 100 °C in an oil bath using a fused $CaCl_2$ guard tube for 15 h. A reddish brown crystalline solid which was precipitated out after 30 min of stirring was isolated by filtration. The isolated product was washed with cold methanol several times and dried under vacuum. A reddish brown crystalline solid was obtained. Yield: 0.45 g, 71%. M.P. −232 °C (decomp.). FT-IR (KBr, cm^{-1}): ν = 2971, 1690, 1661, 1617, 1546, 1516, 1467, 1428, 1373, 1269, 1220, 1119, 1020, 867, 815, 782, 700. ^{1}H-NMR (500 MHz, DMSO-d_6): δ (ppm), 1.09 (t, 12H, NCH_2CH_3, J = 5 Hz), 3.35 (q, 8H, NCH_2CH_3), 6.37–6.35 (q, 2H, xanthene-H, J = 5 Hz), 6.46–6.43 (q, 4H, xanthene-H), 6.67 (d, 1H, phen-H, J = 8 Hz), 6.79 (d, 1H, Ar–H J = 8 Hz), 7.12 (d, 1H, benzo-dioxole-H), 6.79 (d, J = 8 Hz, 1H), 7.12 (d, J = 7.5 Hz, 1H), 7.63–7.59 (q, 2H), 7.93 (d, J = 7.5 Hz, 1H), 9.06 (s, 1H, N═C–H), 9.19 (s, 1H), 10.29 (s, 1H). ^{13}C-NMR (300 MHz, $CDCl_3$ + DMSO-d_6) δ (ppm): 12.87, 44.12, 65.94,

97.84, 105.17, 108.70, 118.23, 119.26, 119.72, 120.74, 123.51, 124.28, 128.14, 129.34, 134.44, 146.00, 146.41, 149.07, 151.65, 153.14, 164.03; ESI-MS: *m*/*z* calculated for $C_{35}H_{37}N_4O_4$ $[M+H]^+$ (*m*/*z*): 577.28, found 577.6. Anal. calc. for $C_{35}H_{36}N_4O_4$: C, 73.02; H, 6.36; N, 9.76; found: C, 72.90; H, 6.29; N, 9.72.

Synthesis of an L–Al^{3+} complex

A 5 mL methanolic solution of $Al_2(SO_4)_3{\cdot}16H_2O$ (0.054 g, 0.0867 mmol) was added dropwise to a magnetically stirred solution (5 mL) of **L** (0.05 g, 0.0867 mmol) in methanol. The color of the ligand solution changed from almost colorless to deep magenta upon addition of $Al_2(SO_4)_3{\cdot}16H_2O$. After two hours of stirring at room temperature, the solution was dried using a rotary evaporator which yielded a magenta **L**–Al^{3+} complex. The complex was characterized by mass spectral studies, FT-IR and ^1H NMR studies.

Crystallographic measurements

Measurements were done on a Bruker SMART APEX II CCD area detector equipped with graphite monochromated Mo Kα radiation (k = 0.71073 Å) source in ω scan mode at 293 K. The structures of the complexes were solved using the SHELXS-97 package of programs and refined by the full-matrix least square technique based on F^2 in SHELXL-97.[21] All non-hydrogen atoms were refined anisotropically. Positions of hydrogen atoms attached to carbon atoms were fixed at their ideal position.

Acknowledgements

A. D. thanks CSIR, New Delhi, India, for financial support by awarding a senior research fellowship (Sanc. No. 01(2401)/10/EMR-II, dated 05.01. 2011).

References

1 For books and reviews: (*a*) A. W. Czarnik, *Fluorescent Chemosensors for Ion and Molecule Recognition*, American Chemical Society, Washington DC, 1993; (*b*) A. P. de Silva, H. Q. N. Gunaratne, T. Gunnlaugsson, A. J. M. Huxley, C. P. McCoy, J. T. Rademacher and T. E. Rice, *Chem. Rev.*, 1997, **97**, 1515; (*c*) B. Valeur and I. Leray, *Coord. Chem. Rev.*, 2000, **205**, 3; (*d*) R. Martínez-Máñez and F. Sancenón, *Chem. Rev.*, 2003, **103**, 4419; (*e*) J. F. Callan, A. P. de Silva and D. C. Magri, *Tetrahedron*, 2005, **61**, 8551; (*f*) L. Basabe-Desmonts, D. N. Reinhoudt and M. Crego-Calama, *Chem. Soc. Rev.*, 2007, **36**, 993.

2 (*a*) M. A. M. Rogers and D. G. Simon, *Age Ageing*, 1999, **28**, 205; (*b*) T. P. Flaten and M. Ødegard, *Food Chem. Toxicol.*, 1988, **26**, 959; (*c*) J. Ren and H. Tian, *Sensors*, 2007, **7**, 3166; (*d*) R. A. Yokel, *Neurotoxicology*, 2000, **21**, 813.

3 (*a*) J. Barcelo and C. Poschenrieder, *Environ. Exp. Bot.*, 2002, **48**, 75; (*b*) Z. Krejpcio and R. W. Pol Wojciak, *J. Environ. Stud.*, 2002, **11**, 251.

4 (*a*) G. D. Fasman, *Coord. Chem. Rev.*, 1996, **149**, 125; (*b*) P. Nayak, *Environ. Res.*, 2002, **89**, 111; (*c*) C. S. Cronan, W. J. Walker and P. R. Bloom, *Nature*, 1986, **324**, 140; (*d*) G. Berthon, *Coord. Chem. Rev.*, 2002, **228**, 319; (*e*) D. R. Burwen, S. M. Olsen, L. A. Bland, M. J. Arduino, M. H. Reid and W. R. Jarvis, *Kidney Int.*, 1995, **48**, 469.

5 K. Soroka, R. S. Vithanage, D. A. Phillips, B. Walker and P. K. Dasgupta, *Anal. Chem.*, 1987, **59**, 629.

6 (*a*) D. Maity and T. Govindaraju, *Inorg. Chem.*, 2010, **49**, 7229; (*b*) D. Maity and T. Govindaraju, *Chem. Commun.*, 2010, **46**, 4499.

7 B. Valeur, *Molecular Fluorescence: Principles and Applications*, Wiley-VCH Verlag GmbH, New York, 2001, ch. 10.

8 (*a*) G. Grynkiewicz, M. Poenie and R. Y. Tsien, *J. Biol. Chem.*, 1985, **260**, 3440; (*b*) A. Minta and R. Y. Tsien, *J. Biol. Chem.*, 1989, **264**, 19449; (*c*) E. Kimura and T. Koike, *Chem. Soc. Rev.*, 1998, **27**, 179.

9 H. Kim, M. Lee, H. Kim, J. Kim and J. Yoon, *Chem. Soc. Rev.*, 2008, **37**, 1465.

10 (*a*) T. Li, R. Fang, B. Wang, Y. Shao, J. Liu, S. Zhang and Z. Yang, *Dalton Trans.*, 2014, **43**, 2741; (*b*) C.-H. Chen, D.-J. Liao, C.-F. Wan and A.-T. Wu, *Analyst*, 2013, **138**, 2527; (*c*) S. H. Kim, H. S. Choi, J. Kim, S. J. Lee, D. T. Quang and J. S. Kim, *Org. Lett.*, 2010, **12**, 560; (*d*) K. K. Upadhyay and A. Kumar, *Org. Biomol. Chem.*, 2010, **8**, 4892; (*e*) Z.-C. Liao, Z.-Y. Yang, Y. Li, B.-D. Wang and Q.-X. Zhou, *Dyes Pigm.*, 2013, **97**, 124.

11 (*a*) S. B. Maity and P. K. Bharadwaj, *Inorg. Chem.*, 2013, **52**, 1161; (*b*) A. Dhara, A. Jana, S. Konar, S. K. Ghatak, S. Ray, K. Das, A. Bandyopadhyay, N. Guchhait and S. K. Kar, *Tetrahedron Lett.*, 2013, **54**, 3630; (*c*) C.-Y. Li, Y. Zhou, Y.-F. Li, C.-X. Zou and X.-F. Kong, *Sens. Actuators, B*, 2013, **186**, 360.

12 (*a*) U. Anthoni, C. Christophersen, P. Nielsen, A. Puschl and K. Schaumburg, *Struct. Chem.*, 1995, **3**, 161; (*b*) Y. Xiang, A. Tong, P. Jin and Y. Ju, *Org. Lett.*, 2006, **8**, 2863.

13 K. A. Connors, *Binding Constants*, Wiley, New York, 1987.

14 R. G. Paar and R. G. Pearson, *J. Am. Chem. Soc.*, 1983, **105**, 7512.

15 W. C. Vosburgh and G. R. Copper, *J. Am. Chem. Soc.*, 1941, **63**, 437.

16 G. L. Long and J. D. Winefordner, *Anal. Chem.*, 1983, **55**, 712A.

17 (*a*) K. Teuchner, A. Pfarrherr, H. Stiel, W. Freyera and D. Leupold, *Photochem. Photobiol.*, 1993, **57**, 465; (*b*) W. Freyer, S. Dahne, L. Q. Minh and K. Teuchner, *Z. Chem.*, 1986, **26**, 334; (*c*) H. Stiel, K. Teuchner, A. Paul, W. Freyer and D. Leupold, *J. Photochem. Photobiol., A*, 1994, **80**, 289.

18 (*a*) J. R. Lakowicz, *Principles of Fluorescence Spectroscopy*, Plenum, New York, 1999; (*b*) A. Jana, P. K. Sukul, S. K. Mandal, S. Konar, S. Ray, K. Das, J. A. Golen, A. L. Rheingold, S. Mondal, T. K. Mondal, A. R. K. Bukhsh and S. K. Kar, *Analyst*, 2014, **139**, 495.

19 R. F. Kubin and A. N. Fletcher, *J. Lumin.*, 1952, **455**, 27.

20 B. Bhattacharya, S. Nakka, L. Guruprasad and A. Samanta, *J. Phys. Chem. B*, 2009, **113**, 2143.

21 G. M. Sheldrick, *Acta Crystallogr. Sect. A*, 2008, **64**, 112.

